



# Spatial Curvature and Thermodynamics

Narayan Banerjee<sup>1</sup> , Purba Mukherjee<sup>2</sup>  and Diego Pavón<sup>3</sup> 

<sup>1</sup>Department of Physical Sciences, Indian Institute of Science Education and Research, Mohanpur, West Bengal - 741246 India

<sup>2</sup>Physics and Applied Mathematics Unit, Indian Statistical Institute, Kolkata - 700108, India

<sup>3</sup>Departamento de Física, Facultad de Ciencias, Universidad Autónoma de Barcelona, 08193 Bellaterra (Barcelona), Spain

Accepted 2023 March 22. Received 2023 March 18; in original form 2023 January 23

## ABSTRACT

Reasonable parametrizations of the current Hubble data set of the expansion rate of our homogeneous and isotropic universe, after suitable smoothing of these data, strongly suggest that the area of the apparent horizon increases irrespective of whether the spatial curvature of the metric is open, flat or closed. Put in another way, any sign of the spatial curvature appears consistent with the second law of thermodynamics.

**Key words:** methods: data analysis – cosmological parameters – cosmology: observations – cosmology: theory

## 1 INTRODUCTION

Homogeneous and isotropic cosmological models are most aptly described by the Friedmann-Lemaître-Robertson-Walker (FLRW) space-time metric,

$$ds^2 = -dt^2 + a^2(t) \left[ \frac{dr^2}{1 - kr^2} + r^2 (d\theta^2 + \sin^2 \theta d\phi^2) \right]. \quad (1)$$

The spatial curvature index,  $k \in \{-1, 0, 1\}$ , indicates whether the spatial part of the metric is open (negatively curved, i.e., hyperbolic), flat, or closed (positively curved).

This constant index, like the scale factor  $a(t)$ , is not a directly observable quantity. In principle, however, it can be determined through the knowledge of the spatial curvature density parameter,  $\Omega_k \equiv -k/(a^2 H^2)$ , which is accessible to observation, albeit indirectly. Recent estimates of the latter, assuming the universe correctly described by the  $\Lambda$ CDM model only suggests that its present absolute value is small ( $|\Omega_{k0}| \sim 10^{-2}$  or less (Komatsu et al. 2011; Ade et al. 2014; Aghanim et al. 2020; Vagnozzi et al. 2021a,b; Dhawan et al. 2021; Park & Ratra 2019; Handley 2021; Mukherjee & Banerjee 2022; Bel et al. 2022; Akarsu et al. 2023)). More recent measurements, not based in the aforesaid model, hint that the universe may not be flat (i.e.,  $k \neq 0$ ) (Park & Ratra 2019; Handley 2021; Mukherjee & Banerjee 2022; Bel et al. 2022). So, the sign of  $k$  is rather uncertain.

Based on the history of the Hubble factor  $H(z)$ , (where  $H = \dot{a}/a$ ) it has been recently argued (Gonzalez-Espinoza & Pavón 2019) that the universe is a thermodynamic system in the sense that it satisfies the second law of thermodynamics (the first law is guaranteed by

Einstein equations while the third law may not apply). As we shall see soon, the possibilities  $k = +1$  and  $k = 0$  are consistent with the second law while this is not so obvious for the third possibility; in principle  $k = -1$  may or may not be compatible with the second law. The aim of our study is to resolve this uncertainty. To this end we shall resort to the 60  $H(z)$  data currently available alongside their  $1\sigma$  confidence intervals, the parametrized graph of this history after smoothing the data set by a Gaussian Process (Rasmussen & Williams 2005), the FLRW metric and the expression of the area of the apparent horizon (Eq. (2) below). As it turns out, the  $k = -1$  possibility (open spatial sections) appears also compatible with the second law of thermodynamics. The paper is organized as follows: In section 2 we write the second law at cosmic scales in terms of the deceleration parameter and  $\Omega_k$ . In section 3 we present the  $H(z)$  data set and the smoothing process. In section 4 we introduce four parametrizations of the Hubble factor and study whether they are compatible with the second law. In section 5 we consider the impact of the Hubble constant priors on our results. Finally, in section 6 we summarize our findings.

As usual, a subindex zero attached at any given quantity indicates that the quantity is to be evaluated at the present epoch. Likewise, we recall, for future convenience, that after fixing  $a_0 = 1$ , the redshift,  $z$ , of any given luminous source is related to the corresponding scale factor by  $1 + z = a^{-1}$ . In our units  $c = G = \hbar = 1$ .

## 2 THE SECOND LAW

Given the strong connection between gravity and thermodynamics (Bekenstein 1974, 1975; Hawking 1974; Jacobson 1995; Padmanabhan 2005), it is natural to expect that the universe behaves as a normal thermodynamic system (Gonzalez-Espinoza & Pavón 2019) whereby it must tend to a state of maximum entropy in the

\* Contact e-mail: [narayan@iiserkol.ac.in](mailto:narayan@iiserkol.ac.in)

† Contact e-mail: [purba16@gmail.com](mailto:purba16@gmail.com)

‡ Contact e-mail: [diego.pavon@uab.es](mailto:diego.pavon@uab.es)

**Table 1.** Recent Hubble parameter compilation from cosmic chronometers.

$z$	$H(z)$ [km Mpc <sup>-1</sup> s <sup>-1</sup> ]	Ref.
0.09	69 ± 12	
0.17	83 ± 8	
0.27	77 ± 14	
0.4	95 ± 17	
0.48	97 ± 62	
0.88	90 ± 40	Stern et al. (2010)
0.9	117 ± 23	
1.3	168 ± 17	
1.43	177 ± 18	
1.53	140 ± 14	
1.75	202 ± 40	
0.1797	75 ± 4	
0.1993	75 ± 5	
0.3519	83 ± 14	
0.5929	104 ± 13	Moresco et al. (2012)
0.6797	92 ± 8	
0.7812	105 ± 12	
0.8754	125 ± 17	
1.037	154 ± 20	
0.07	69.0 ± 19.6	
0.12	68.6 ± 26.2	Zhang et al. (2014)
0.2	72.9 ± 29.6	
0.28	88.8 ± 36.6	
1.363	160.0 ± 33.6	Moresco (2015)
1.965	186.5 ± 50.4	
0.3802	83.0 ± 13.5	
0.4004	77.0 ± 10.2	
0.4247	87.1 ± 11.2	Moresco et al. (2016)
0.4497	92.8 ± 12.9	
0.4783	80.9 ± 9	
0.47	89 ± 49.6	Ratsimbazafy et al. (2017)
0.75	98.8 ± 33.6	Borghi et al. (2022)

long run (Radicella & Pavon 2012; Pavon & Radicella 2013).

A basic standpoint is that the entropy of the universe is dominated by entropy of the cosmic horizon. In fact its entropy ( $\sim 10^{132}k_B$ ) exceeds by far the combined entropies of super-massive black holes, the cosmic microwave background radiation, the neutrino sea, etc (Egan & Lineweaver 2010). As cosmic horizon, we take the apparent horizon rather than other possible choices, since the laws of thermodynamics are fulfilled on it (Wang et al. 2006). Its entropy (proportional to its area) is given by  $S_{\mathcal{A}} = k_B \pi \tilde{r}_{\mathcal{A}}^2 / \ell_P^2$  (Bak & Rey 2000; Cai 2008), with  $\tilde{r}_{\mathcal{A}} = (H^2 + k a^{-2})^{-1/2}$  as the radius of the horizon.

Obviously, the area of the apparent horizon,

$$\mathcal{A} = \frac{4\pi}{H^2 + \frac{k}{a^2}}, \quad (2)$$

depends on the Hubble factor and spatial curvature.

By the second law of thermodynamics  $S'_{\mathcal{A}} \geq 0$ , thus

$$\mathcal{A}' = -\frac{\mathcal{A}^2}{8\pi^2} \left( HH' - \frac{k}{a^3} \right) \geq 0 \quad \Rightarrow \quad HH' \leq \frac{k}{a^3}, \quad (3)$$

where the prime indicates  $d/da$ .

**Table 2.** Recent Hubble parameter compilation from the radial BAO & galaxy clustering.

$z$	$H(z)$ [km Mpc <sup>-1</sup> s <sup>-1</sup> ]	$r_d^{\text{fid}}$ [Mpc]	Ref.
0.24	79.69 ± 2.99		
0.34	83.8 ± 3.66	153.3	Gaztanaga et al. (2009)
0.43	86.45 ± 3.97		
0.44	82.6 ± 7.8		
0.6	87.9 ± 6.1	–	Blake et al. (2012)
0.73	97.3 ± 7		
0.3	81.7 ± 6.22	152.76	Oka et al. (2014)
0.35	82.7 ± 9.1	152.76	Chuang & Wang (2013)
0.57	96.8 ± 3.4	147.28	Anderson et al. (2014)
0.31	78.17 ± 4.74		
0.36	79.93 ± 3.39		
0.40	82.04 ± 2.03		
0.44	84.81 ± 1.83		
0.48	87.79 ± 2.03	147.74	Wang et al. (2017)
0.52	94.35 ± 2.65		
0.56	93.33 ± 2.32		
0.59	98.48 ± 3.19		
0.64	98.82 ± 2.99		
0.38	81.5 ± 1.9		
0.51	90.4 ± 1.9	147.78	Alam et al. (2017)
0.61	97.3 ± 2.1		
0.978	113.72 ± 14.63		
1.23	131.44 ± 12.42		
1.526	148.11 ± 12.71	147.78	Zhao et al. (2019)
1.944	172.63 ± 14.79		
2.33	224 ± 8	147.33	Bautista et al. (2017)
2.34	222 ± 7	147.7	Delubac et al. (2015)
2.36	226 ± 8	147.49	Font-Ribera et al. (2014)

The above inequality tells us: (i) if  $H'$  is or has been positive at any stage of cosmic expansion (excluding, possibly, the pre-Planckian era), then  $k = +1$ , (ii)  $H' < 0$  may, in principle, be compatible with any sign of  $k$ , and (iii) the possibilities  $k = +1$  and  $k = 0$  are consistent with the second law. In particular the data analysis carried out by the 2018 Planck mission produced the 99% probability region  $-0.095 < \Omega_{k0} < -0.007$  on the spatial curvature parameter (Aghanim et al. 2020). Note that this bound on  $\Omega_{k0}$  is fully compatible with the second law because it corresponds to the possibility  $k = +1$ . However, the third possibility,  $k = -1$ , may or may not be compatible.

The inequality  $HH' \leq \frac{k}{a^3}$  can be recast as

$$1 + q \geq \Omega_k, \quad (4)$$

where  $q = -\ddot{a}/(aH^2) = -(1 + \dot{H}H^{-2})$  is the deceleration parameter.

Equation (4) expresses the second law of thermodynamics at cosmic scales (Gonzalez-Espinoza & Pavón 2019).

To see that it is perfectly reasonable, let us assume the universe dominated by a perfect fluid of energy density  $\rho$  and hydrostatic pressure  $P$ . The corresponding Einstein equations can be written as,

$$H^2 + \frac{k}{a^2} = \frac{8\pi}{3}\rho \quad \text{and} \quad \frac{\ddot{a}}{a} = -\frac{4\pi}{3}(\rho + 3P). \quad (5)$$

If the fluid is dust ( $P = 0$ ), one has  $q > 0$ , and these equations lead

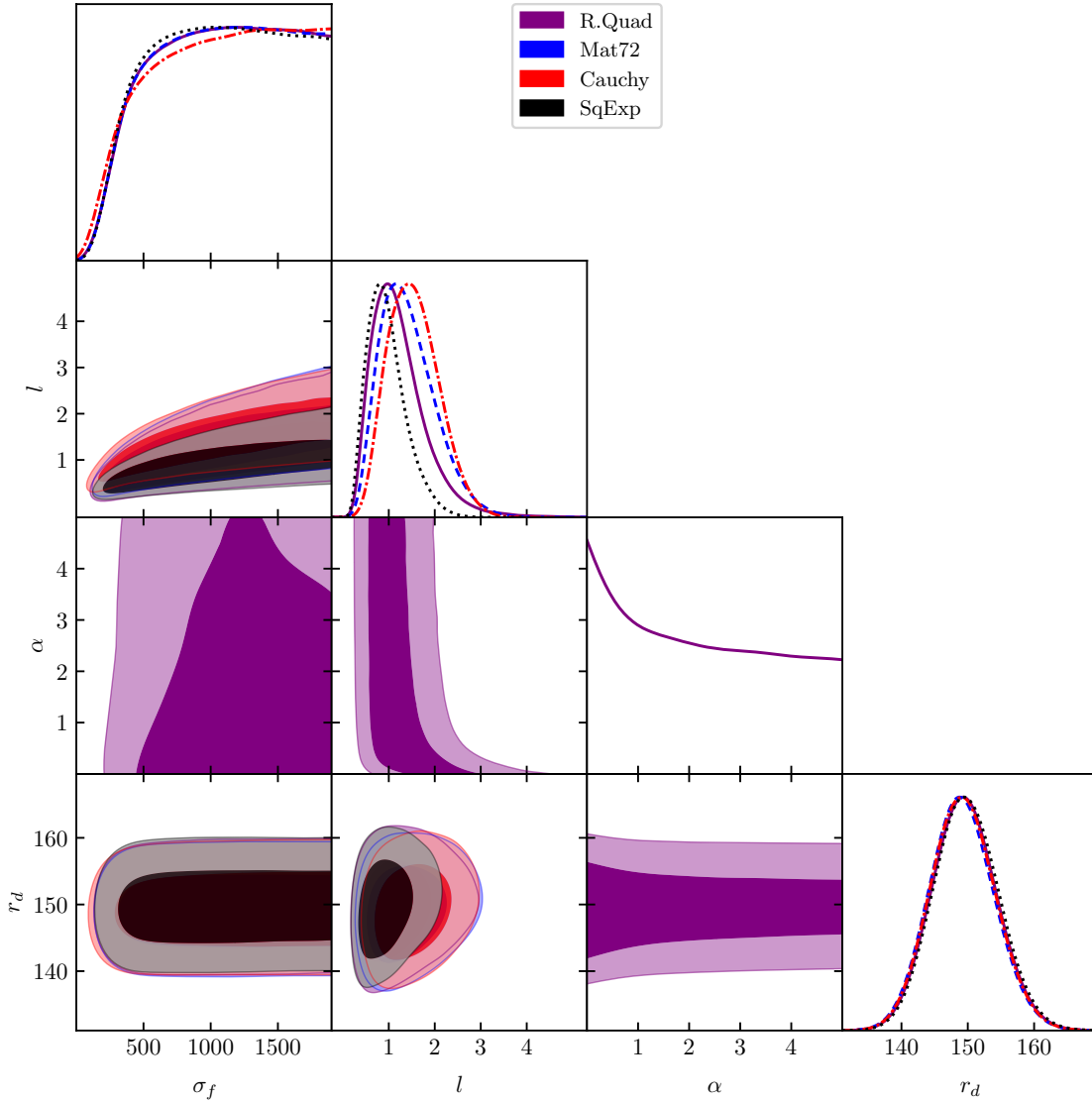


**Figure 1.** Contour plots for GP hyperparameter space and the comoving sound horizon at drag epoch whose radius,  $r_d$ , is measured in megaparsecs.

to  $\Omega_k = 1 - 2q$ .

If the second law holds, i.e.,  $1 + q \geq \Omega_k$ , it follows that  $q \geq 0$  which is consistent with the fact that a pressureless matter dominated universe decelerates ( $q > 0$ ).

By contrast, should the second law not hold,  $1 + q < \Omega_k$ , the absurd result  $0 < -q$  (namely, zero less than a negative quantity), would follow.

Likewise, if the equation of state of the fluid filling the universe were  $P = w\rho$  with  $w \geq -1$  the expression  $1 + q \geq \Omega_k$  also proves to be consistent with the corresponding sign of the deceleration parameter and not so, if  $1 + q < \Omega_k$ . Values of  $w$  lower than  $-1$  correspond to phantom fields. As is well known these fields are unstable both classically (Dabrowski 2015) and quantum

mechanically<sup>1</sup> (Cline et al. 2004).

Further, by combining the Friedmann equation in the case of a universe dominated by pressureless matter, the cosmological constant and spatial curvature with the acceleration equation (5.b), we obtain

$$\frac{\ddot{a}}{a} - \left(\frac{\dot{a}}{a}\right)^2 - \frac{k}{a^2} = -4\pi\rho_m. \quad (6)$$

The latter can be rewritten as

$$1 + q = \Omega_k + \frac{3}{2}\Omega_m \quad (\Omega_m = 8\pi\rho_m/(3H^2)), \quad (7)$$

which makes apparent the reasonableness of the expression  $1 + q \geq \Omega_k$ . Moreover, the above shows the compatibility of the said expression with general relativity.

<sup>1</sup> Should  $H'$  be positive, the FLRW universe could neither be flat nor open, just closed ( $k = +1$ ) which would be puzzling in view of the current data that clearly allow for  $k = 0$ .

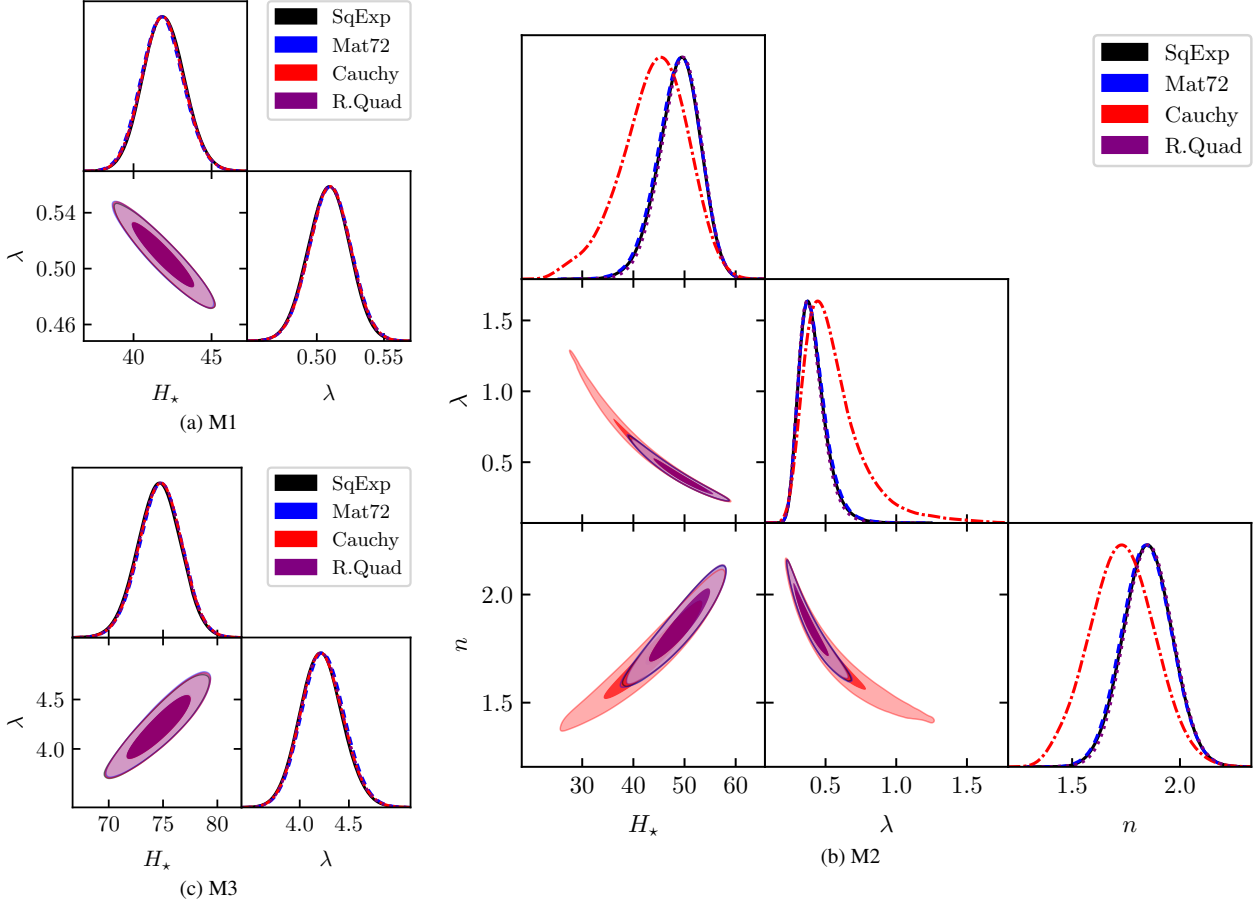


**Figure 2.** Contour plots for (a) first  $H(a)$  model parameters, (b) second  $H(a)$  model parameters, and (c) third  $H(a)$  model parameters, using different choices of the GP kernel, where  $H_*$  is in units of  $\text{km Mpc}^{-1} \text{s}^{-1}$ .

### 3 HUBBLE DATA SET AND SMOOTHING PROCESS

Our data set consists of: (i) recent 32 cosmic chronometer (CC)  $H(z)$  measurements, presented in Table 1, which do not assume any particular cosmological model, and (ii) the 28  $H(z)$  measurements from baryon acoustic oscillations (BAO) from different galaxy surveys, listed in Table 2. In both cases, the datasets are given with their  $1\sigma$  confidence interval. Because the BAO measurements are not entirely model-independent, particularly due to the assumption of a fiducial radius of the comoving sound horizon,  $r_d^{\text{fid}}$ , we adopted a full marginalization over the GP hyperparameter space (see below) with the comoving sound horizon at drag epoch  $r_d$  for the BAO data set as free parameter. This results in a model-independent Hubble data set from CC and the calibrated BAO.

As is apparent, a handful of  $H(z)$  data are afflicted by a rather large  $1\sigma$  confidence intervals whence some statistically founded

smoothing process must be applied to the full data set to arrive to sensible results. This is why we resort to the machine-learning model Gaussian Process (GP) which infers a function from labelled training data (Rasmussen & Williams 2005; Seikel et al. 2012), and reconstruct the Hubble diagram as a function of the scale factor. The said process is able to reproduce an ample range of behaviors with just a few parameters and allows a Bayesian interpretation (Zhao et al. 2008). Then, after smoothing the Hubble data set, we constrain the free parameters that enter the proposed parametric expressions (Eqs. (10), (13) and (15), below) of the history of the Hubble factor and check whether the corresponding curves,  $H(a)$ , are consistent with the second law. That is to say, whether they comply with the inequality  $1 + q \geq \Omega_k$ .

To undertake the GP, we consider the squared exponential (SqExp hereafter), Matérn 7/2 (Mat72 hereafter), Cauchy and rational quadratic (R.Quad hereafter) covariance functions,

$$k(a, \tilde{a}) = \begin{cases} \sigma_f^2 \exp\left(-\frac{(a-\tilde{a})^2}{2l^2}\right) & \dots \text{Sq.Exp,} \\ \sigma_f^2 \exp\left(-\frac{7|a-\tilde{a}|}{l}\right) \left[1 + \frac{7|a-\tilde{a}|}{l} + \frac{14(a-\tilde{a})^2}{5l^2} + \frac{7\sqrt{7}|a-\tilde{a}|^3}{15l^3}\right] & \dots \text{Mat.72,} \\ \sigma_f^2 \left[\frac{l}{(a-\tilde{a})^2 + l^2}\right]^{-\alpha} & \dots \text{Cauchy,} \\ \sigma_f^2 \left[1 + \frac{(a-\tilde{a})^2}{2\alpha l^2}\right]^{-\alpha} & \dots \text{R.Quad,} \end{cases} \quad (8)$$

**Table 3.** Parameter values for the first (M1) parametrization corresponding to each kernel, where  $H_\star$  and  $H_0$  are in units of  $\text{km Mpc}^{-1} \text{ s}^{-1}$ .

$k(a, \tilde{a})$	$H_\star$	$\lambda$	$H_0$	$q_0$	$a_t$
Sq.Exp	$41.926^{+1.332}_{-1.292}$	$0.509^{+0.015}_{-0.015}$	$69.751^{+1.229}_{-1.211}$	$-0.488^{+0.014}_{-0.013}$	0.509
Mat.7/2	$41.818^{+1.345}_{-1.311}$	$0.510^{+0.015}_{-0.016}$	$69.622^{+1.274}_{-1.267}$	$-0.487^{+0.014}_{-0.014}$	0.510
Cauchy	$41.879^{+1.339}_{-1.304}$	$0.510^{+0.015}_{-0.015}$	$69.712^{+1.273}_{-1.258}$	$-0.487^{+0.014}_{-0.014}$	0.510
R.Quad	$41.893^{+1.340}_{-1.303}$	$0.509^{+0.015}_{-0.015}$	$69.722^{+1.289}_{-1.260}$	$-0.488^{+0.014}_{-0.014}$	0.509

**Table 4.** Parameter values for the second (M2) parametrization, where  $H_\star$  and  $H_0$  are in units of  $\text{km Mpc}^{-1} \text{ s}^{-1}$ .

$k(a, \tilde{a})$	$H_\star$	$\lambda$	$n$	$H_0$	$q_0$	$a_t$
Sq.Exp	$49.107^{+3.835}_{-4.247}$	$0.397^{+0.104}_{-0.077}$	$1.849^{+0.113}_{-0.113}$	$68.664^{+1.477}_{-1.563}$	$-0.469^{+0.044}_{-0.047}$	0.556
Mat.7/2	$48.973^{+3.927}_{-4.361}$	$0.401^{+0.108}_{-0.079}$	$1.845^{+0.115}_{-0.114}$	$68.626^{+1.538}_{-1.543}$	$-0.468^{+0.045}_{-0.047}$	0.555
Cauchy	$44.486^{+5.934}_{-6.967}$	$0.513^{+0.232}_{-0.142}$	$1.731^{+0.152}_{-0.151}$	$67.317^{+2.063}_{-2.084}$	$-0.447^{+0.068}_{-0.073}$	0.567
R.Quad	$49.342^{+3.762}_{-4.121}$	$0.392^{+0.100}_{-0.075}$	$1.855^{+0.112}_{-0.111}$	$68.692^{+1.494}_{-1.520}$	$-0.472^{+0.044}_{-0.045}$	0.554

**Table 5.** Parameter values for the third (M3) parametrization corresponding to each kernel, where  $H_\star$  and  $H_0$  are in units of  $\text{km Mpc}^{-1} \text{ s}^{-1}$ .

$k(a, \tilde{a})$	$H_\star$	$\lambda$	$H_0$	$q_0$	$a_t$
Sq.Exp	$74.635^{+1.938}_{-1.970}$	$4.215^{+0.216}_{-0.210}$	$74.750^{+1.772}_{-1.770}$	$-0.842^{+0.020}_{-0.019}$	0.546
Mat.7/2	$74.798^{+1.928}_{-1.964}$	$4.237^{+0.220}_{-0.212}$	$74.917^{+1.791}_{-1.721}$	$-0.847^{+0.020}_{-0.018}$	0.544
Cauchy	$74.751^{+1.931}_{-1.975}$	$4.224^{+0.221}_{-0.210}$	$74.878^{+1.806}_{-1.779}$	$-0.846^{+0.020}_{-0.019}$	0.545
R.Quad	$74.735^{+1.922}_{-1.978}$	$4.225^{+0.218}_{-0.210}$	$74.862^{+1.763}_{-1.752}$	$-0.846^{+0.020}_{-0.019}$	0.545

(also called “kernels”) where  $\sigma_f$ ,  $l$  and  $\alpha$  are the hyperparameters. Throughout this work, we assume a zero mean function to characterize the GP. We investigate if the different covariance functions lead to significant differences in the results<sup>2</sup>.

We adopt a python implementation of the ensemble sampler for MCMC, the emcee<sup>3</sup>, introduced by Foreman-Mackey et al. (2013). The two dimensional confidence contours showing the uncertainties along with the one dimensional marginalized posterior probability distributions, are shown in Fig. 1 with the help of the GetDist<sup>4</sup> module of python, developed by Lewis (2019).

#### 4 PARAMETRIZATIONS

In this section we study whether hyperbolic, i.e., open, spatial sections (which correspond to  $k = -1$ ) are compatible with the second law of thermodynamics as expressed by Eq. (4). To this end we consider three parametrizations (equations (10), (13) and (15), below) of the history of the Hubble factor and use the corresponding parameter values obtained after the smoothing of the Hubble data (tables 3, 4 and 5 for the first, second and third parametrizations, respectively<sup>5</sup>). Figure 2 shows the contour plots

of the different parameters occurring the three parametrizations. Then we check whether the corresponding curves,  $H(a)$ , comply with the inequality (4). These curves are shown in Fig. 3.

We express  $\Omega_k$  as

$$\Omega_k = \Omega_{k0} \left( \frac{a_0 H_0}{a H} \right)^2, \quad (9)$$

with  $\Omega_{k0} \lesssim 10^{-2}$  the upper bound on the likely present value of the spatial curvature parameter assuming  $k = -1$ , see Komatsu et al. (2011); Ade et al. (2014); Park & Ratra (2019); Handley (2021); Mukherjee & Banerjee (2022); Bel et al. (2022).

In the cases considered below  $H_\star \equiv H(a \rightarrow \infty)$ . The analysis of the fourth parametrization does not call for a numerical study.

Before going any further, it is worthwhile to note that since  $0 < \Omega_{k=-1} < 1$  and that  $q > 0$  ( $< 0$ ) when the universe is decelerating (accelerating), the said inequality cannot be violated when the universe is decelerating.

##### 4.1 First parametrization

A reasonable and simple parametrization of the Hubble factor in an ever-expanding FLRW universe, regardless of the spatial curvature (M1 hereafter), is

$$H = H_\star \exp(\lambda/a), \quad (10)$$

<sup>2</sup> For details on GP, visit <http://www.gaussianprocess.org>

<sup>3</sup> <https://github.com/dfm/emcee>

<sup>4</sup> <https://github.com/cmbant/getdist>

<sup>5</sup> In these tables  $a_t$  is the scale factor at which the transition from deceleration to acceleration occurs.

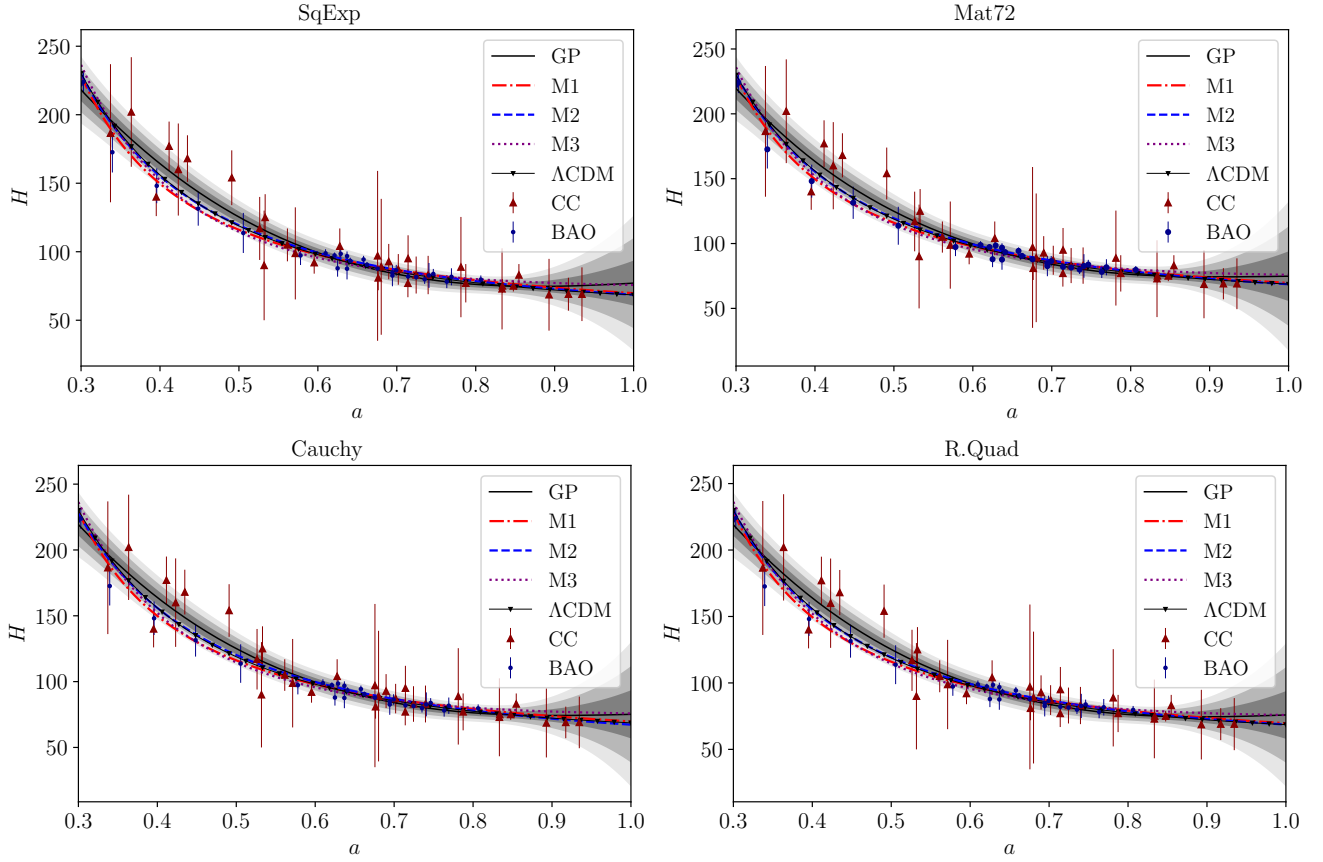


**Figure 3.** Plots for  $H(a)$ , in units of  $\text{km Mpc}^{-1} \text{s}^{-1}$ , with their  $1\sigma$ ,  $2\sigma$  and  $3\sigma$  confidence intervals vs  $a$  for different choices of the GP kernel, where M1, M2 and M3 denote the first, second and third  $H(a)$  parametrizations, respectively.

where  $H_\star$  and  $\lambda$  are free parameters to be fitted to the data by means of the GP method.

Since  $1+q = \lambda/a$  there is deceleration when  $a < \lambda$  and acceleration when  $a > \lambda$ . On the other hand, recalling that  $\Omega_k$  is given by (9), and after setting  $a_0 = 1$ , Eq. (4) boils down to

$$\frac{\lambda}{a} \geq \Omega_{k0} \frac{\exp[2\lambda(\frac{a-1}{a})]}{a^2}, \quad (11)$$

which can be rewritten as

$$\zeta_{M1} = \lambda a \exp\left[2\lambda\left(\frac{1}{a} - 1\right)\right] \geq \Omega_{k0}. \quad (12)$$

Using the best fit values of  $H_\star$  and  $\lambda$ , shown in Table 3 corresponding to each kernel, we find that  $\zeta_{M1}$  stays above  $\Omega_{k0}$  in the full range, (0.3, 1), of the scale factor covered by the data as shown in Fig. 4. Thus Eq. (12) is satisfied, i.e., the curve  $H(a)$  of the first parametrization respects, by a comfortable margin, the second law of thermodynamics also if  $k = -1$ .

## 4.2 Second parametrization

A somewhat less simple parametrization (M2 hereafter) is

$$H = H_\star(1 + \lambda a^{-n}). \quad (13)$$

This one contains three free parameters, namely,  $H_\star$ ,  $\lambda$  and  $n$ , to be fitted to the data. Proceeding as before we can write,

$$\zeta_{M2} = \lambda \frac{(\lambda + a^n)}{[(1 + \lambda) a^{n-1}]^2} \geq \Omega_{k0}. \quad (14)$$

Using the best fit values of  $\lambda$  and  $n$  displayed in table 4 we see, as Fig. 4 shows, that last equation is fulfilled (and therefore Eq. (4)) by an ample margin in the whole interval of the scale factor currently observationally accessible. Again, the second law is respected even if  $k = -1$ .

## 4.3 Third parametrization

Similarly, consider the expression (M3 hereafter) for the Hubble rate

$$H(a) = \frac{H_\star}{1 - \exp(-\lambda a^2)}, \quad (15)$$

where  $H_\star$  and  $\lambda$  are free parameter to be fit to the data.

Proceeding as in the previous cases from equations (4) and (9) we obtain

$$\zeta_{M3} = 2 \frac{\lambda(1 - \exp(-\lambda))^2 a^4}{(1 - \exp(-\lambda a^2))^3} \geq \Omega_{k0}. \quad (16)$$

As before, resorting to the best fit values of the free parameters as given in table 5 it is seen, that the above equation is satisfied (and consequently Eq. (4) as well) by a generous margin in the whole



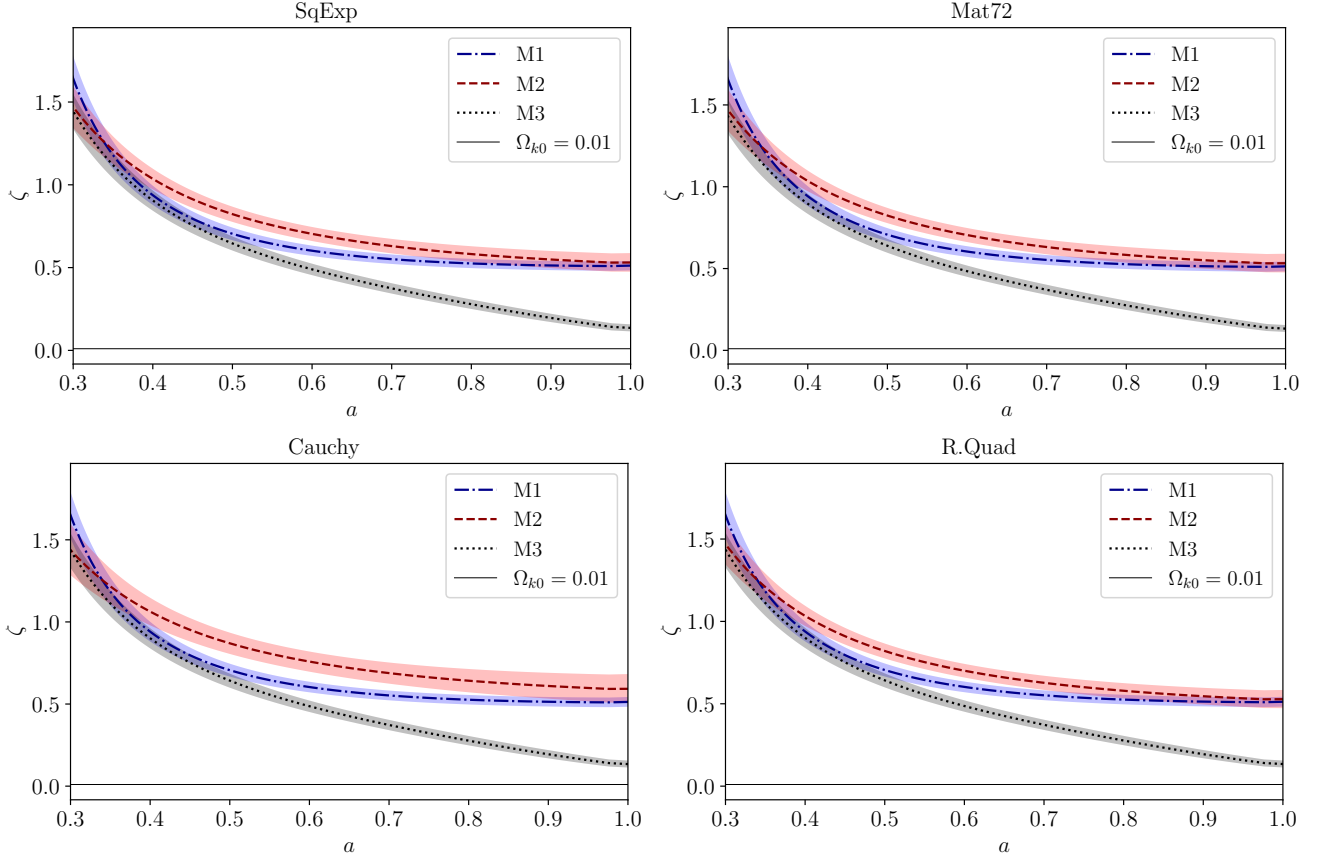


**Figure 4.** Plots for  $\zeta$  with their  $1\sigma$  confidence interval vs  $a$  for different choices of the GP kernel, where M1, M2 and M3 denotes the first, second and third  $H(a)$  parametrizations, respectively. Every single curve stays above of the observational upper bound of  $\Omega_{k0}$ ,  $\sim 10^{-2}$ , in the whole scale factor interval.

interval of the scale factor observationally accessible, as shown in Fig. 4. Once again, the second law is respected even if  $k = -1$ .

#### 4.4 Fourth parametrization

Consider the expression for the Hubble factor inspired in the  $\Lambda$ CDM model

$$H(a) = H_0 \sqrt{\Omega_{m0} a^{-3} + \Omega_{k0} a^{-2} + \Omega_{\Lambda}}, \quad (17)$$

where  $H_0$ ,  $\Omega_{m0}$  and  $\Omega_{\Lambda}$  are free parameters. Following parallel steps to the previous cases, we write  $\zeta_{M4} = \frac{1}{2} (3\Omega_{m0} a^{-1} + 2\Omega_{k0}) \geq \Omega_{k0}$ , that is to say

$$\zeta_{M4} = \frac{3}{2} \Omega_{m0} a^{-1} \geq 0. \quad (18)$$

It is immediately seen that Eq. (4) is satisfied for whatever value of the scale factor and consequently the second law as well.

## 5 EFFECT OF $H_0$ PRIORS

We further examine to what extent (if at all) the rising tension between the local measurements of the Hubble constant (Riess et al. 2022; Freedman 2021), and its inferred values via an extrapolation of data on the early universe (Aghanim et al. 2020) affects our results.

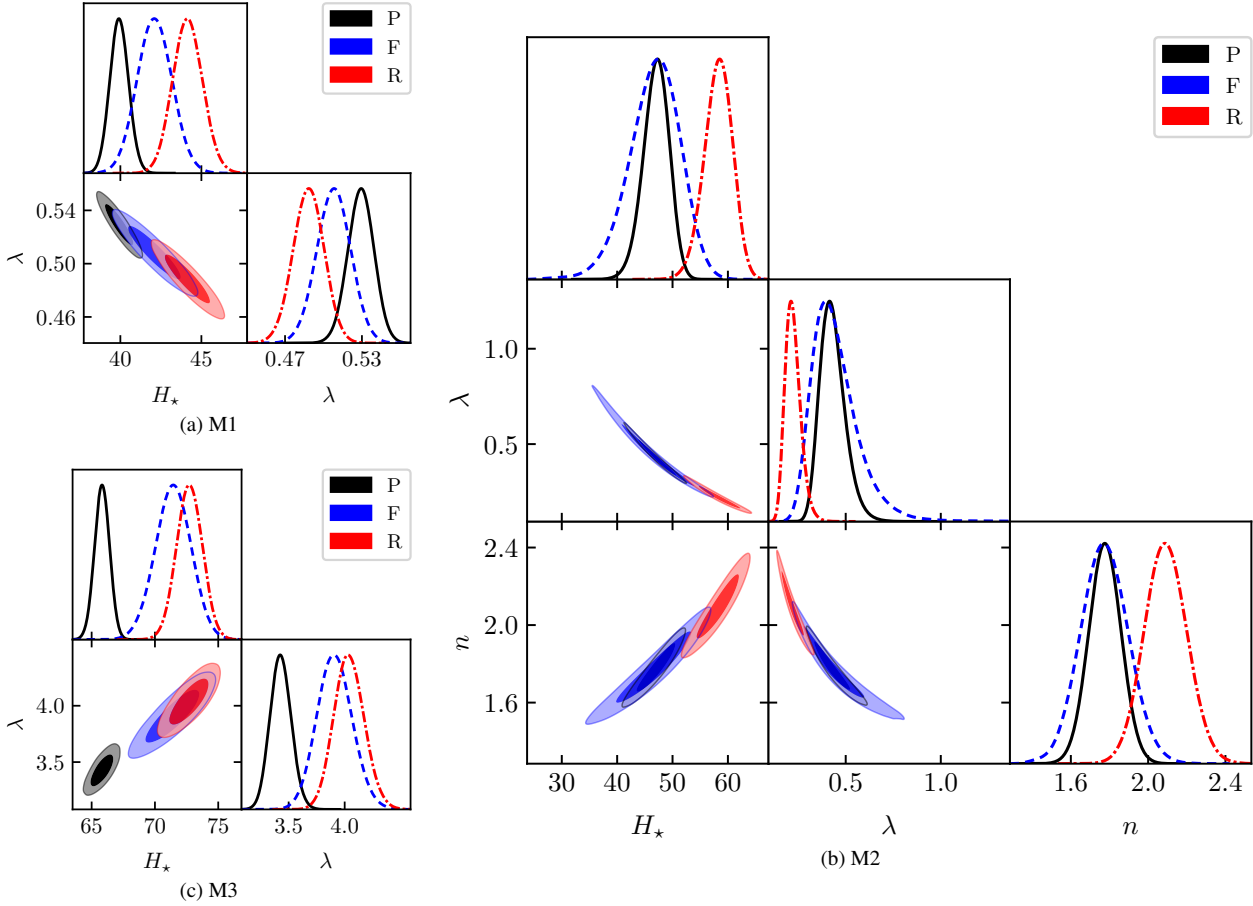
To this end we consider (i) the local measurements by the SH0ES team [ $H_0^{\text{R22}} = 73.3 \pm 1.04 \text{ km Mpc}^{-1} \text{ s}^{-1}$  (R hereafter)], (ii) the updated TRGB calibration from the Carnegie Supernova Project [ $H_0^{\text{F21}} = 69.8 \pm 1.7 \text{ km Mpc}^{-1} \text{ s}^{-1}$  (F hereafter)], and (iii) the inferred value via an extrapolation of data on the early universe by the Planck survey [ $H_0^{\text{P20}} = 67.4 \pm 0.5 \text{ km Mpc}^{-1} \text{ s}^{-1}$  (P hereafter)], respectively. We assume Gaussian prior distributions with the mean and variances corresponding to the best-fit and  $1\sigma$  confidence interval reported about  $H_0$  values.

Fig. 5 shows the contour plots of the different parameters occurring in the three parametrizations, on assuming these  $H_0$  values. The constraints on the parameter values are given in Tables 6, 7, and 8, for the first, second and third parametrizations. The corresponding  $H(a)$  and  $\zeta$  curves are shown in Figs. 6 and 7, respectively.

We can conclude this section by saying that our overall result, that the constrain  $1 + q \geq \Omega_k$  is satisfied even if  $k = -1$ , is not affected whether we take the  $H_0$  value from the local measurements or the one obtained from extrapolating the precise data drawn from the cosmic microwave background radiation.

## 6 CONCLUDING REMARKS

The second law of thermodynamics applied to our expanding FLRW universe implies that the area of its apparent horizon cannot decrease, i.e.,  $\mathcal{A}' \geq 0$ . This, in its turn, dictates  $HH' \leq k/a^3$ .



**Figure 5.** Contour plots for (a) first  $H(a)$  model parameters, (b) second  $H(a)$  model parameters, and (c) third  $H(a)$  model parameters, using P20, F21 and R22  $H_0$  values as priors, where  $H_\star$  is in units of  $\text{km Mpc}^{-1} \text{s}^{-1}$ .

**Table 6.** Parameter values for the first (M1) parametrization corresponding to the three  $H_0$  values as priors, where  $H_\star$  and  $H_0$  are in units of  $\text{km Mpc}^{-1} \text{s}^{-1}$ .

Prior	$H_\star$	$\lambda$	$H_0$	$q_0$	$a_t$
P	$39.927^{+0.579}_{-0.566}$	$0.529^{+0.010}_{-0.010}$	$67.778^{+0.466}_{-0.458}$	$-0.468^{+0.010}_{-0.010}$	0.529
F	$42.111^{+1.078}_{-1.058}$	$0.508^{+0.013}_{-0.013}$	$69.965^{+1.013}_{-1.001}$	$-0.489^{+0.012}_{-0.012}$	0.508
R	$44.144^{+0.928}_{-0.910}$	$0.488^{+0.012}_{-0.012}$	$71.937^{+0.797}_{-0.795}$	$-0.509^{+0.011}_{-0.012}$	0.489

**Table 7.** Parameter values for the second (M2) parametrization corresponding to the three  $H_0$  values as priors, where  $H_\star$  and  $H_0$  are in units of  $\text{km Mpc}^{-1} \text{s}^{-1}$ .

Prior	$H_\star$	$\lambda$	$n$	$H_0$	$q_0$	$a_t$
P	$47.105^{+2.216}_{-2.408}$	$0.426^{+0.070}_{-0.058}$	$1.776^{+0.083}_{-0.083}$	$67.194^{+0.477}_{-0.500}$	$-0.465^{+0.031}_{-0.030}$	0.536
F	$46.948^{+4.256}_{-4.774}$	$0.428^{+0.133}_{-0.095}$	$1.774^{+0.123}_{-0.121}$	$67.081^{+1.321}_{-1.379}$	$-0.464^{+0.054}_{-0.051}$	0.535
R	$58.330^{+2.417}_{-2.607}$	$0.219^{+0.043}_{-0.036}$	$2.090^{+0.111}_{-0.108}$	$71.126^{+0.904}_{-0.917}$	$-0.619^{+0.034}_{-0.033}$	0.504

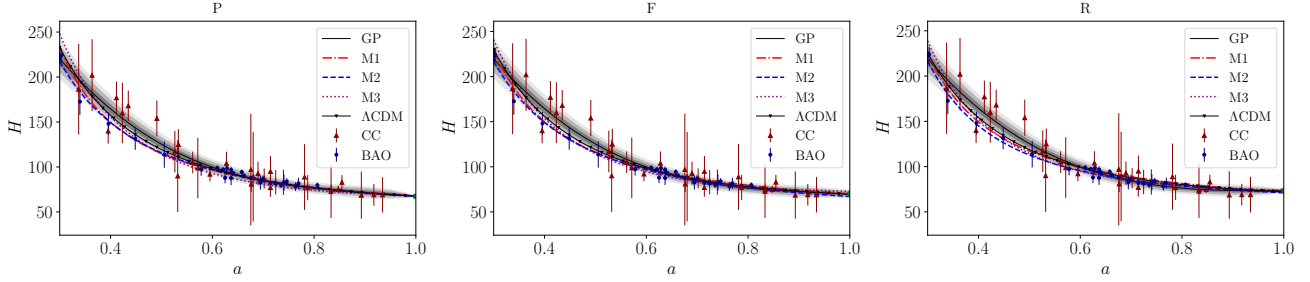
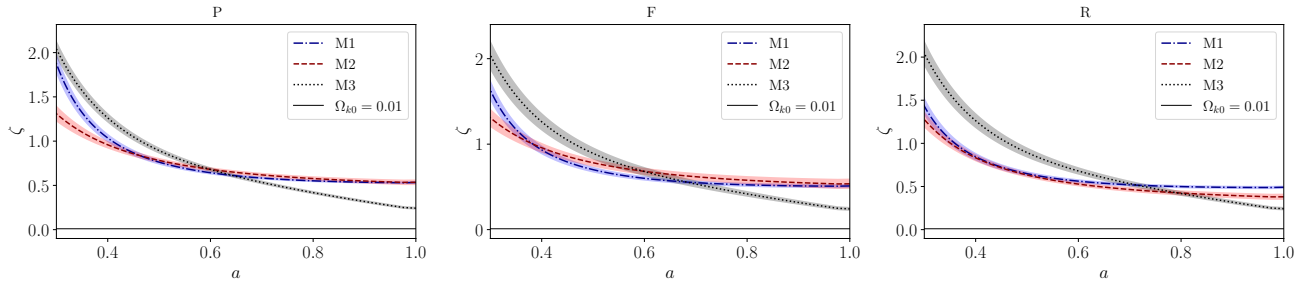
Since in absence of phantom fields, which are unstable,  $H' < 0$  leads to two possibilities, namely,  $k = 0$  and  $k = +1$ , result immediately compatible with the second law. The third possibility,  $k = -1$ , may or may not be compatible with it. Here we resorted to the set of observational data regarding the evolution of the Hubble factor to discern whether the said law is satisfied when  $k = -1$ . So, with the help of the non-parametric Gaussian Process

we smoothed the set of 60 currently available data of the Hubble factor and introduced four different parametrizations of the ensuing curve,  $H(a)$ . After using the latter to constrain the free parameters entering the first three parametrizations (the fourth one was not in need of a numerical study), we examined whether the resulting expressions, with the curvature index  $k$  fixed to  $-1$ , satisfy Eq. (4). As it turned out, all of them did (Fig. 4 and Eq. (18)). Further,



**Table 8.** Parameter values for the third (M3) parametrization corresponding to the three  $H_0$  values as priors, where  $H_\star$  and  $H_0$  are in units of  $\text{km Mpc}^{-1} \text{ s}^{-1}$ .

Prior	$H_\star$	$\lambda$	$H_0$	$q_0$	$a_t$
P	$65.824^{+0.589}_{-0.590}$	$3.427^{+0.094}_{-0.091}$	$68.032^{+0.477}_{-0.483}$	$-0.758^{+0.015}_{-0.016}$	0.605
F	$71.444^{+1.393}_{-1.402}$	$3.909^{+0.158}_{-0.152}$	$72.925^{+1.230}_{-1.245}$	$-0.830^{+0.017}_{-0.019}$	0.567
R	$72.722^{+1.014}_{-1.009}$	$4.037^{+0.136}_{-0.130}$	$74.025^{+0.914}_{-0.901}$	$-0.845^{+0.014}_{-0.014}$	0.558


**Figure 6.** Plots for  $H(a)$ , in units of  $\text{km Mpc}^{-1} \text{ s}^{-1}$ , with their  $1\sigma$ ,  $2\sigma$  and  $3\sigma$  confidence intervals vs  $a$  using P20, F21 and R22  $H_0$  values as priors (from left to right), where M1, M2 and M3 denotes the first, second and third  $H(a)$  parametrizations, respectively.

**Figure 7.** Plots for  $\zeta$  with their  $1\sigma$  confidence interval vs  $a$  using P20, F21 and R22  $H_0$  values as priors (from left to right), where M1, M2 and M3 denote the first, second and third  $H(a)$  parametrizations, respectively.

a quick inspection of the said expressions shows that they also comply with Eq. (4) in the limit  $a \rightarrow \infty$ . Therefore, we are led to conclude that the evolution of FLRW universes with open spatial sections does not appear to conflict with the second law of thermodynamics. Regrettably, a final verdict cannot be attained at this stage since currently we have no cosmological model that deserves our unreserved confidence. In fact, the most reliable model, the so-called ‘‘concordance model’’, is afflicted by some drawbacks whose relevance may not be small (Perivolaropoulos & Skara 2022; Di Valentino 2022). This is why we did resort to parametrize the Hubble factor rather than taking it from any given model.

One may argue that this conclusion could be reached from Eq.(7) straightaway. However this is not so because that equation only concerns the adiabatic evolution of the fluid that sources the gravitational field. Further, the second law does not enter its derivation whereby it cannot be ascertained whether it is respected or violated.

## ACKNOWLEDGMENTS

PM thanks ISI Kolkata for financial support through Research Associateship.

## DATA AVAILABILITY

Authors can confirm that all relevant source data are included in the article. The data sets generated during and/or analysed during this study are available from the corresponding author on reasonable request.

## REFERENCES

- Ade P. A. R., et al., 2014, *Astron. Astrophys.*, 571, A16
- Aghanim N., et al., 2020, *Astron. Astrophys.*, 641, A6
- Akarsu O., Di Valentino E., Kumar S., Ozyigit M., Sharma S., 2023, *Phys. Dark Univ.*, 39, 101162
- Alam S., et al., 2017, *Mon. Not. Roy. Astron. Soc.*, 470, 2617
- Anderson L., et al., 2014, *Mon. Not. Roy. Astron. Soc.*, 441, 24
- Bak D., Rey S.-J., 2000, *Class. Quant. Grav.*, 17, L83
- Bautista J. E., et al., 2017, *Astron. Astrophys.*, 603, A12
- Bekenstein J. D., 1974, *Phys. Rev. D*, 9, 3292
- Bekenstein J. D., 1975, *Phys. Rev. D*, 12, 3077
- Bel J., Larena J., Maartens R., Marinoni C., Perrenon L., 2022, *JCAP*, 09, 076
- Blake C., et al., 2012, *Mon. Not. Roy. Astron. Soc.*, 425, 405
- Borghesi N., Moresco M., Cimatti A., 2022, *Astrophys. J. Lett.*, 928, L4
- Cai R.-G., 2008, *Progress of Theoretical Physics Supplement*, 172, 100
- Chuang C.-H., Wang Y., 2013, *Mon. Not. Roy. Astron. Soc.*, 435, 255
- Cline J. M., Jeon S., Moore G. D., 2004, *Phys. Rev. D*, 70, 043543

- Dabrowski M. P., 2015, *Eur. J. Phys.*, 36, 065017
- Delubac T., et al., 2015, *Astron. Astrophys.*, 574, A59
- Dhawan S., Alsing J., Vagnozzi S., 2021, *Mon. Not. Roy. Astron. Soc.*, 506, L1
- Di Valentino E., 2022, *Universe*, 8, 399
- Egan C. A., Lineweaver C., 2010, *Astrophys. J.*, 710, 1825
- Font-Ribera A., et al., 2014, *JCAP*, 05, 027
- Foreman-Mackey D., Hogg D. W., Lang D., Goodman J., 2013, *Publ. Astron. Soc. Pac.*, 125, 306
- Freedman W. L., 2021, *Astrophys. J.*, 919, 16
- Gaztanaga E., Cabre A., Hui L., 2009, *Mon. Not. Roy. Astron. Soc.*, 399, 1663
- Gonzalez-Espinoza M., Pavón D., 2019, *Mon. Not. Roy. Astron. Soc.*, 484, 2924
- Handley W., 2021, *Phys. Rev. D*, 103, L041301
- Hawking S. W., 1974, *Nature*, 248, 30
- Jacobson T., 1995, *Phys. Rev. Lett.*, 75, 1260
- Komatsu E., et al., 2011, *Astrophys. J. Suppl.*, 192, 18
- Lewis A., 2019, [arXiv:1910.13970](https://arxiv.org/abs/1910.13970)
- Moresco M., Cimatti A., Jimenez R., Pozzetti L., et al., 2012, *JCAP*, 2012, 006
- Moresco M., 2015, *Mon. Not. Roy. Astron. Soc.*, 450, L16
- Moresco M., et al., 2016, *JCAP*, 05, 014
- Mukherjee P., Banerjee N., 2022, *Phys. Rev. D*, 105, 063516
- Oka A., Saito S., Nishimichi T., Taruya A., Yamamoto K., 2014, *Mon. Not. Roy. Astron. Soc.*, 439, 2515
- Padmanabhan T., 2005, *Phys. Rept.*, 406, 49
- Park C.-G., Ratra B., 2019, *Astrophys. Space Sci.*, 364, 134
- Pavon D., Radicella N., 2013, *Gen. Rel. Grav.*, 45, 63
- Perivolaropoulos L., Skara F., 2022, *New Astron. Rev.*, 95, 101659
- Radicella N., Pavon D., 2012, *Gen. Rel. Grav.*, 44, 685
- Rasmussen C. E., Williams C. K. I., 2005, *Gaussian Processes for Machine Learning*. The MIT Press, doi:10.7551/mitpress/3206.001.0001, <https://doi.org/10.7551/mitpress/3206.001.0001>
- Ratsimbazafy A. L., Loubser S. I., Crawford S. M., Cress C. M., Bassett B. A., Nichol R. C., Väisänen P., 2017, *Mon. Not. Roy. Astron. Soc.*, 467, 3239
- Riess A. G., et al., 2022, *Astrophys. J. Lett.*, 934, L7
- Seikel M., Clarkson C., Smith M., 2012, *JCAP*, 06, 036
- Stern D., Jimenez R., Verde L., Kamionkowski M., Stanford S. A., 2010, *JCAP*, 02, 008
- Vagnozzi S., Di Valentino E., Gariazzo S., Melchiorri A., Mena O., Silk J., 2021a, *Phys. Dark Univ.*, 33, 100851
- Vagnozzi S., Loeb A., Moresco M., 2021b, *Astrophys. J.*, 908, 84
- Wang B., Gong Y., Abdalla E., 2006, *Phys. Rev. D*, 74, 083520
- Wang Y., et al., 2017, *Mon. Not. Roy. Astron. Soc.*, 469, 3762
- Zhang C., Zhang H., Yuan S., Zhang T.-J., Sun Y.-C., 2014, *Res. Astron. Astrophys.*, 14, 1221
- Zhao G.-B., et al., 2019, *Mon. Not. Roy. Astron. Soc.*, 482, 3497
- Zhao K., Popescu S., Zhang X., 2008, *Photogrammetric Engineering & Remote Sensing*, 74, 1223

This paper has been typeset from a  $\mathrm{T}_{\mathrm{E}}\mathrm{X}/\mathrm{L}^{\mathrm{A}}\mathrm{T}_{\mathrm{E}}\mathrm{X}$  file prepared by the author.